RESEARCH



Expression of costimulatory molecule CD70 is prognostic in small cell lung cancer

David Dora¹ · Zsolt Megyesfalvi^{2,3,4} · Imre Vörös^{5,6,7,8} · Ágnes Paál^{5,6,7,8} · Peter Takacs¹ · Daniela Dobos¹ · Bence Lőrincz¹ · Syeda Mahak Zahra Bokhari⁹ · Kenan Aloss^{9,12} · Gergely Pallag¹ · Christopher Rivard¹⁰ · Hui Yu¹⁰ · Fred R. Hirsch^{10,11} · Anikó Görbe^{5,6} · Zoltán V. Varga^{6,7,8} · Zoltan Lohinai⁹ · Balazs Dome^{2,3,4}

Received: 11 December 2024 / Accepted: 1 March 2025 © The Author(s) 2025

Abstract

Introduction Small cell lung cancer (SCLC) is a highly aggressive malignancy with poor survival outcomes. The CD70-CD27 axis has been implicated in immune regulation and tumor progression across cancers, but its role in SCLC has not yet been elucidated. This research explores the expression patterns and prognostic significance of CD70 and CD27 in early-stage SCLC.

Methods In this retrospective study, we analyzed 190 surgically resected SCLC tumor samples using immunohistochemistry (IHC) for CD70 and CD27 expression and RNAscope for CD70 RNA detection. Immune infiltration was assessed using CD45, CD8, and CD20 staining. Quantification of RNAscope signals was performed using QPath software. Kaplan–Meier survival analysis and multivariate Cox regression were used to assess the prognostic impact of CD70, CD27, and immune cell infiltrates on overall survival (OS).

Results CD70 was expressed in 46% of tumors, primarily within tumor nests, with lower expression in stromal areas. High CD70 expression correlated with significantly decreased OS (p=0.0078, HR: 1.795) without any correlation with CD45+, CD8+ or CD20+ immune cell infiltrates. CD27 expression was mainly confined to the stroma, and it did not show a significant association with OS (p=0.582). Importantly, high CD27 expression was linked to reduced CD45+ and CD8+ cell densities in the stroma. Both CD70 and CD27 were expressed on CD68+ macrophages, CD27 was expressed on CAFs, and both molecules exhibited a partial coexpression with CD3. Furthermore, patients with high CD20+B-cell densities or the presence of tertiary lymphoid structures (TLS) had significantly improved OS (p=0.0017, HR: 0.491), suggesting the importance of B-cell-related immune responses in SCLC prognosis.

Conclusion CD70, B-cell density and the presence of TLSs, but not CD27, emerged as a significant prognostic biomarker for OS in surgically treated SCLC, suggesting its potential as a therapeutic target.

Keywords Small-cell lung cancer · CD70 · CD27 · B-cell · TLS · Tumor microenvironment

Introduction

Small cell lung cancer (SCLC) is a highly aggressive malignancy. Conventional efforts to repurpose established biomarkers and conduct clinical trials have yielded consecutive failures. Immunotherapy has recently improved the 5-year survival rate of advanced-stage non-small cell lung cancer (NSCLC) patients from 5 to 23.2% [16]. In SCLC, immune checkpoint inhibitor (ICI) combinations have been

Zoltan Lohinai and Balazs Dome share last authorship.

Published online: 09 April 2025

Extended author information available on the last page of the article

approved, including the IMpower133 and CASPIAN regimens. However, despite these advancements, the clinical benefit remains incremental, with median overall survival gains of approximately two months, and long-term survival improvements are limited [24], [41]). While historically, the 5-year overall survival (OS) rate for advanced-stage SCLC has remained below 1%, recent data from the IMbrella extension study report a 12% 5-year OS rate for patients receiving carboplatin, etoposide, and atezolizumab [59].

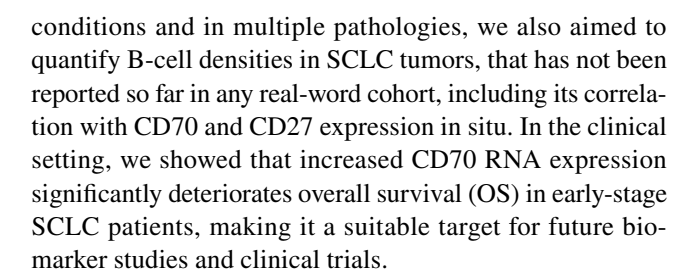
CD70 and CD27 are a ligand-receptor pair, that belong to the tumor necrosis factor (TNF) superfamily [15]. CD27 is found primarily on memory B and T cells, as well as naive T cells, and some subsets of natural killer cells. In



physiological conditions, tightly controlled expression of CD70 and CD27 plays a role in co-stimulation in immune response. CD27 activation by CD70 induces a cleavage of the CD27 extracellular domain, and can be also detected as a fragment (sCD27) in bodily fluids [27, 28], [48]. However, its role in the tumor microenvironment (TME) is far more multifaceted [15], [51]. Dysregulation of the CD70-CD27 axis within the tumor and its microenvironment is associated with tumor progression and immunosuppression [15]. Interestingly, abnormally high levels of sCD27 have been found to be present in patients presenting with a hematological malignancy, which suggests the involvement of the CD70-CD27 axis [54], [56]; [20], [48]). Tumor cells regulate CD27 expression in the TME by expressing CD70, which promotes immune escape [34]. Furthermore, CD27 signaling increases regulatory T cell (Treg cell)-infiltration promoting tumor growth [9].

The CD70-CD27 axis plays a key role in hematopoiesis. CD27 is present on murine progenitor cells [37] and CD70 inhibits leukocyte differentiation via CD27 activation [37]. Targeting this axis has been explored in hematological neoplasms, including Hodgkin lymphoma, diffuse large B-cell lymphoma [4, 43], and chronic- [49] and acute myeloid leukemia ([47]; [50]). In multiple myeloma, CD27 expression decreases with disease progression [22]. However, in the last decade, the therapeutic prospect of the CD70-CD27 axis has gained more significance in solid tumors as well. Its indubious role has been elicited in renal cell carcinoma ([10]; [29]), ovarian carcinoma [35], pleural mesothelioma [25], breast cancer [42], malignant melanoma [44], and NSCLC [27, 28]. In glioblastoma multiforme (GBM), CD70 plays a key role in recurrent GBM cell aggressiveness and maintenance. In SCLC, it was reported that immune cell infiltration and expression of immune checkpoints and other immunostimulatory molecules, including IDO, PVR or STING are increased in the neuroendocrine-low (or variant) subtype [11], the latter identified as a positive prognosticator along with CD8+immune cell infiltration [13]. Furthermore, RNAseq data on a subcohort of n = 30 earlystage SCLC patients showed that CD70 is overexpressed in the more immunogenic NE-low subtype of SCLC [12]. To date, no data is available on the tissue expression pattern and prognostic role of the CD70/CD27 axis in SCLC.

In the current study, we analyzed the RNA and protein expression of CD70, using RNAscope and immunofluorescence (IF) and the protein expression of its receptor, CD27, including its correlation with CD45 + CD8 + immune cell infiltration previously reported in [13] on a large, realword cohort of early-stage SCLC patients. Furthermore, we quantified the tissue expression of CD70's receptor, CD27 in the TME and its colocalizing expression signals with tumor- stromal and immune cells. Because the CD70/CD27 axis is heavily involved in B-cell biology in physiological



Materials and methods

Ethical statement

The study was carried out in accordance with the Helsinki Declaration guidelines of the World Medical Association Hungarian scientific ethics committee (ETT-TUKEB-7214–1/2016/EKU). Due to the retrospective nature of the study, the requirement for individual informed consent was waived. Following the acquisition of clinical data, the patients' identities were anonymized, ensuring that the patients cannot be identified either directly or indirectly.

Study population

In this retrospective study, 190 surgically-resected and histologically confirmed consecutive SCLC patients were included between 1975 and 2013 at the National Koranyi Institute of Pulmonology, Budapest, Hungary. The study and all treatments were conducted based on the institutional guidelines. The date of the last follow-up included in this analysis was April 2022. Clinicopathological data included age, gender, disease stage and details concerning adjuvant chemotherapy and overall survival (OS). Table 1 shows

Table 1 Clinicopathological characteristics of the cohort with available clinical data according to CD70 expression (high vs low)

Clinical characteristic	CD70-High	CD70-Low	<i>p</i> -value*
Stage I/II	28 (73.7%)	21 (63.6%)	0.443
Stage III	10 (26.3%)	12 (36.4%)	
Gender (Female)	31 (81.6%)	25 (75.8%)	0.574
Gender (Male)	7 (18.4%)	8 (24.2%)	
Adjuvant CT (Yes)	23 (60.5%)	18 (54.5%)	0.637
Adjuvant CT (No)	15 (39.5%)	15 (45.5%)	
Overall survival (median, months)	12.6	33.3	0.02
Age (median, years)	57.0	58.0	0.583

P values for Mann Whitney U test in case of continuous variables and Chi-squared test in case of categorical varibles. Percentages refer to the percent of total patients with available clinical data stained for CD70



clinicopathological characteristics for patients with available clinical data according to CD70 expression (high vs low).

Tissue processing

Following surgery, SCLC tumor samples underwent fixation and were subsequently processed into paraffin blocks. The construction of tissue microarrays (TMAs) from formalinfixed paraffin-embedded (FFPE) blocks was conducted in accordance with established methods [3]. In brief, 4-micron sections were meticulously sliced from each tissue block using an HM-315 microtome (Microm) and deposited onto charged glass slides (Colorfrost Plus, #22–230-890, Fisher). These slides were subjected to hematoxylin and eosin (H&E) staining using an automated Tissue-Tek Prisma staining platform (Sukura). An experienced pathologist, certified in thoracic oncology, examined the H&E-stained slides to identify the tumor area, demarcating its boundaries. Two 1-mm tissue punches were extracted from each donor tissue block and precisely positioned into a recipient paraffin block, arranged in an encoded array format using an MP10 1.0-mm tissue punch on a manual TMA instrument (Beecher Instruments).

Immunohistochemistry and immunofluorescence

For the immunohistochemistry (IHC), five-micron-thick sections were prepared. The staining was carried out on a Leica Bond RX autostainer with rabbit monoclonal antibodies against CD20 (#48,750) from Cell Signaling and CD27 (#131,254) from abcam, diluted to 1:200 following the protocols established by [13]. Briefly, after primary antibody binding sites visualization, slides underwent staining with the Bond Polymer Refine Detection kit (#DS9800) following Leica IHC Protocol F. Epitope retrieval 1 (low pH) was conducted for 20 min. Hematoxylin was used for counterstaining. For dual Immunofluorescence (IF) stainings, we used antibodies against CD70 (#300,083), CD27 (#131,254), CD68 (#201,340), and CD3 (#201,340) from abcam and CD20 (#14-0202-82) and Vimentin (VIM, #MA5-11,883) from Invitrogen, each at a 1:200 dilution in 1% PBS/BSA. Dual immunofluorescence (IF) employed Alexa IgG antirabbit A488 and IgG anti-mouse A546 fluorescent secondary antibodies from Invitrogen for detecting signals from CD70, CD27, CD3, CD20, CD68, and VIM antibodies. Autofluorescence on FFPE samples was eliminated with TrueView® Autofluorescence Quencher (Vector). Human tonsil and lung adenocarcinoma tissues served as positive controls for protein expression assessment.

RNAscope

The RNAScope® ISH assay was executed on tissue microarrays (TMAs) employing the RNAScope® Multiplex

Fluorescent Kit v2 in accordance with the manufacturer's protocols (Advanced Cell Diagnostics Pharma Assay Services, Newark, CA, USA) and as previously described [14]. Briefly, 4 µm sections of formalin-fixed paraffin-embedded TMA were pretreated with antigen-retrieval buffer, heat, and protease. Subsequently, hybridization was performed with the following target oligo probes: 3plex-Hs-Positive Control Probe (ACDBio, cat: 320,861), 3plex-Hs-Negative Control Probe (ACDBio, cat: 320,871), and Hs-CD70 (ACDBio, Cat No. 419331). Preamplifier, amplifier, and AMP-labeled oligo probes were then sequentially hybridized, followed by the development of fluorogenic precipitates (Cy3, red). Each sample underwent quality control to assess RNA integrity using a positive control probe specific to housekeeping genes, and a negative control probe set was employed to evaluate background fluorescence. Nuclei were counterstained using 4',6-diamidino-2-phenylindole (DAPI).

Scoring the CD70 RNAscope signal with QPath

To quantitatively assess RNA expression, we employed the Opath software package, following established methods and equations to quantify the dotted fluorescent signals in our regions of interest (ROIs) ([2]; [14]. Briefly, we employed DAPI nuclear staining to delineate individual cell regions by assigning each cell's radius, designating each cell as a region of interest (ROI). Subsequently, we quantified the number of dots within each ROI, following established procedures. An integrated expression score within the [0–3] range was calculated for all tumor cores, based on the average density of dots and raw intensity data. The determination of cutoffs was performed using the k-means clustering method. For all tissue microarrays (TMAs), two cores per patient were included, and an average CD70 expression score was computed for each patient. The median value for aggregate CD70 scores was 2.0. To ensure balanced classification of CD70 "high vs "low" tumors, we decided to include tumors scoring 2.0 to the CD70 "high group. All intensity measurements were conducted utilizing an LSM780 Zeiss confocal microscope and Zen Blue software package.

Scoring of CD20 and CD27 expression

Images of TMA sections were captured for scoring and cell counting using a BX53 upright Olympus microscope equipped with a DP74 color CMOS camera at $10 \times$ magnification in 20MP resolution, and representative images from tumor tissues were captured at $20 \times$ magnification. For all TMAs, two cores per patient were included. From all TMA blocks, two separate four-micron-thick sections, spaced at least $100 \, \mu m$ apart in the Z-axis, were quantified. The ImageJ software package was used to perform cell counting, where microscopical images of sectioned and stained TMA cores were imported



and followed by conversion to an 8-bit grayscale format to enhance contrast. The "Threshold" function was used to define and isolate the cells from the background, with adjustments averaged using 100 images manually counted to yield an accuracy of $\pm 5\%$. Adjustments were made to ensure proper identification of individual cells. Subsequently, the "Analyze Particles" feature was utilized to count the cells, with size and circularity parameters set to exclude debris or cell clusters, using the above-mentioned averaging. A macro was then created and applied to all samples. The results were then recorded as the total number of cells per BLANK.

Datasets

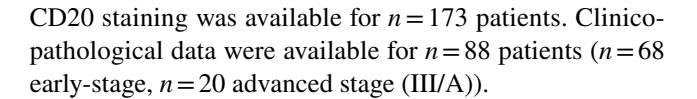
To assess the single-cell expression pattern of the CD70/ CD27 axis in the healthy lung, we used the Human Protein Atlas (HPA, http://www.proteinatlas.org/, [53]). To evaluate CD70 and CD27 expression in the TME of lung cancer, Broad Institute's Single Cell Portal was used compiling data from Zilionis et al. [58], where a comprehensive scRNAseq profiling of myeloid and lymphoid TME cell populations was carried out on n=7 NSCLC patient samples. RNA-seq data are reported as average fragments per kilobase of exon per million reads mapped (FPKM) for both datasets used. Single cell expression levels of major cell types and the proprietary LM22 immune cell set was used to assess the expression pattern of the axis in human lung cancers. LM22 is a signature matrix file distinguishing 22 mature human hematopoietic populations isolated from peripheral blood or in vitro culture conditions [7].

Statistical analyses

Normality was evaluated using the Shapiro–Wilk test and nonparametric Mann–Whitney U-test was used for cell density comparisons. Comparison of TLS presence with CD70 and CD27 phenotype was performed using the chi-squared test. Survival analysis was performed with Kaplan–Meier curves and a comparison of survival curves with the log-rank test. Cox-proportional hazard regression was used to screen for significant predictor variables. The analysis was two-sided with a level of significance of α =0.05. To assess the goodness of fit of our multivariate model, Harrel's C-index (>0.7) was calculated. Violin charts were visualized using GraphPad Prism 8.0 and KM-curves were generated with the MedCalc 14 statistical software package.

Results

A total of n = 190 patients were included in our study with resected SCLC of whom n = 167 patients had scoreable CD70 RNAscope stainings and n = 182 CD27 stainings.



The CD70/CD27 axis is expressed in healthy lung and lung cancer

According to single-cell data retrieved from the Human Protein Atlas (HPA), costimulatory molecules CD70 and CD28 are both expressed in the healthy lung. CD70 is mainly expressed in B-cells, and in plasma cells in line with the molecule's biology in healthy hosts, with considerable expression in Langerhans- and T-cells, basal respiratory cells and fibroblasts as well (SFig 1A). CD27 is predominantly expressed in plasma cells, but also in B-cells, with notable expression levels in T-cells and erythroid populations (SFig 1B) according to HPA data, suggesting the lympho-myeloid dominance of the axis in physiological conditions. In the healthy lung, based on single-cell data, CD70 is expressed in B-cells and two distinct T-cell populations, with a minor presence on macrophages. Club cells and endothelial cell populations also show traces of CD70 expression (SFig 1C). CD27 is predominantly expressed in B- and T-cells with a small addition from different macrophage populations (SFig 1D).

Data retrieved from the SingleCell (SC) portal suggest that CD70 and CD27 are also expressed in the TME of NSCLC. 1 from 7 patients showed high-, 3 from 7 showed modest CD70 expression when observing all cell types (Fig. 1A). In contrast 6 from 7 patients exhibited moderateto-high CD27 expression levels (Fig. 1B). When observing single-cell expression levels specifically for major cell types and LM22 cell populations, it is shown that CD70 is mostly expressed in B-cell populations and plasma cells, and in CD4+T-cells (both naive and memory), regulatory T-cells (T-regs) and eosinophils to a smaller extent (Fig. 1C, E, and F). CD27 shows the most prominent expression in plasma cells, where a considerable percentage of the cell type's cells express the protein, but also T-regs, follicular helper T-cells and other CD4+T-cell populations show notable expression of CD27 (Fig. 1D,E and G).

Expression of CD70 and CD27 in SCLC

RNA Expression scores were established for each patient based on RNAscope assays and an area-adjusted quantitative scoring system using QPath. Panels in Fig. 2A-C show representative images of strong (score = 3), moderate (score = 2) and low (score = 1) expression levels for CD70. CD70 RNA signals were predominantly located in tumor nests (Fig. 2A,B dashed line areas), but also scattered in stroma (Fig. 2A arrows). Histograms of CD70 score distribution through patients show similar to normal distribution



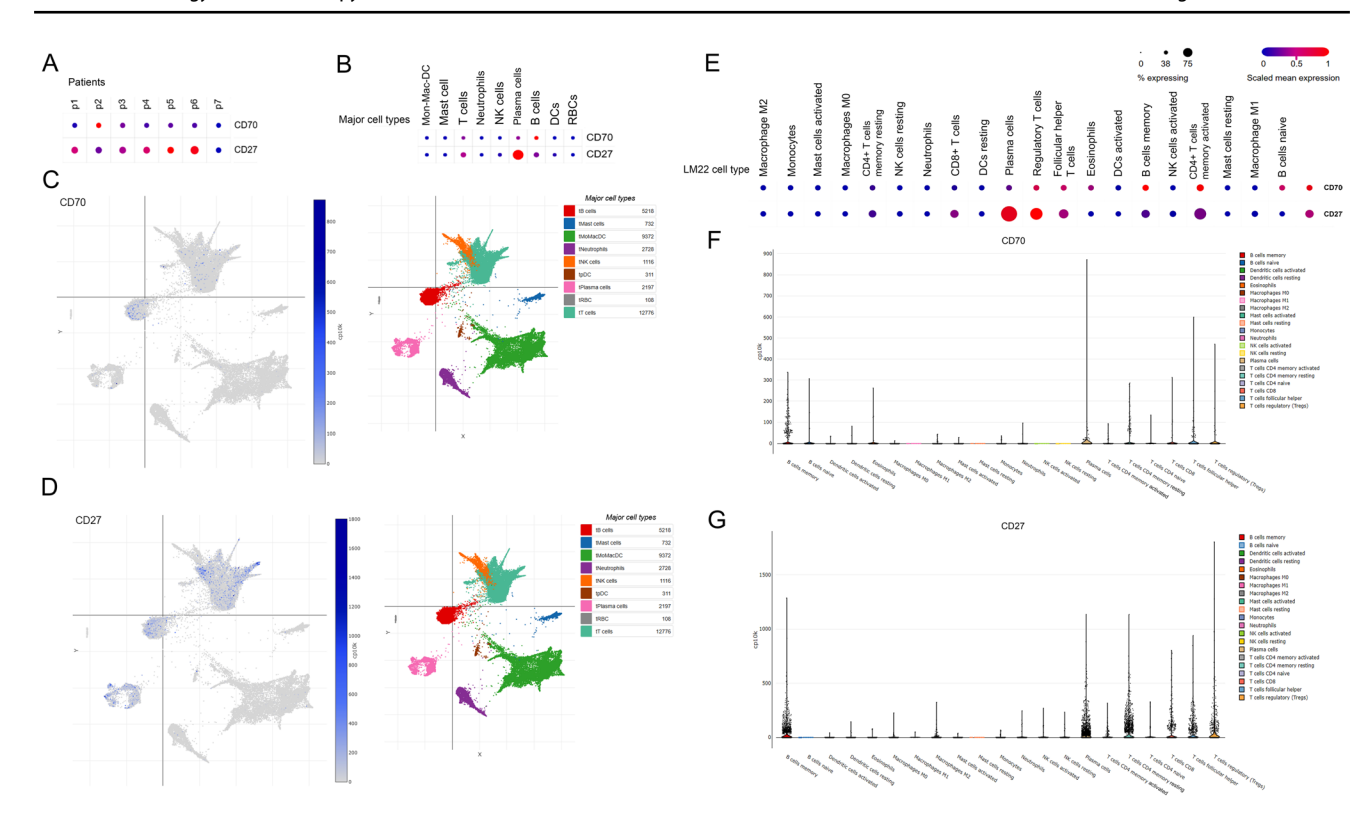


Fig. 1 Expression of the CD70-CD27 axis in NSCLC. Single-cell data from the SingleCell portal show expression means and percentage of expressing cells in dot plots comparing CD70 and CD27, according to included patients (**A**) and major cell types (**B**). UMAP plots show the number and cluster of cells expressing CD70 (**C**) and CD27 (**D**). CD70 is expressed in B-cells, CD4+T-cells (naive, memory), T-regs, and eosinophils within the NSCLC tumor microenviron-

ment according to the LM22 signature matrix file (**E**, **F**). CD27 is primarily expressed in plasma cells, T-regs, follicular helper T-cells, and other CD4+T-cell populations based on the same dataset (**E**, **G**). Row minimums and maximums (RNA expression, Log(CP10k+1) normalized counts matrix (genes by cells)) in panel A are color coded. Size of corresponding circles correlates with the percentage of expressing cells for every cell type in dot plots

with most tumors scoring 1.0–2.0 (Fig. 2D). All tumors with aggregate values of 2.0–3.0 were classified as CD70 "high", and with values of 0–1.5 were classified as CD70 "low." Next, we compared CD45 + immune cell- and CD8 + T-cell densities separately in the stroma and tumor nest compartments according to CD70 expression using data published earlier in the same cohort [13]. It is shown that CD70 RNA expression is not associated significantly with immune cell infiltrates neither in the stroma (Fig. 2E,G), nor in the tumor nest compartments (Fig. 2F,H). Thus, high CD70 expression does not come with categorically higher- or lower immune cell densities.

Expression of CD27 was evaluated on the same cohort using an IHC-based quantitative scoring system described earlier [11],2022). CD27 is expressed predominantly in the stroma compartment (Fig. 2I,J), which was confirmed using RNAscope as well (Fig. 2K,L) Histogram shows the distribution of tumors according to CD27+cellular densities (Fig. 2M). In contrast with CD70, it is shown that high CD27 expression was associated with decreased CD45+(Fig. 2N) and CD8+cellular densities (Fig. 2P), but only in the stroma compartment, not in tumor nests (Fig. 2O,Q). Neither CD70

expression (rs = -0.0421, p = 0.713), nor CD27 + cellular density (rs = 0.0165, p = 0.881) show significant correlation with tumor stage, suggesting an expression pattern inherent to the original tumor phenotype.

B-cells and tertiary lymphatic structures (TLSs) in SCLC

We also evaluated CD20+B-cell densities in our SCLC cohort. Representative images show tumor TMAs with low (Fig. 3A) and relatively high (Fig. 3B) B-cell densities. As expected, B-cells are mostly located in stromal bands, but also occur intratumorally and occasionally create congregations known as TLSs. We identified a total of n = 14 patients (8%) with TLS present in their tumors, as shown in stainings on Fig. 3C and D. When comparing CD20+B-cell densities with the expression of CD70 and CD27, we found no significant association between the immunomodulatory molecules and B-cell densities (Fig. 3E-H) neither in stroma nor inside tumor nests. We came to the similar conclusion, when assessing the presence of TLSs along with CD70- and CD27 expression in the same cohort (Fig. 3J,K).





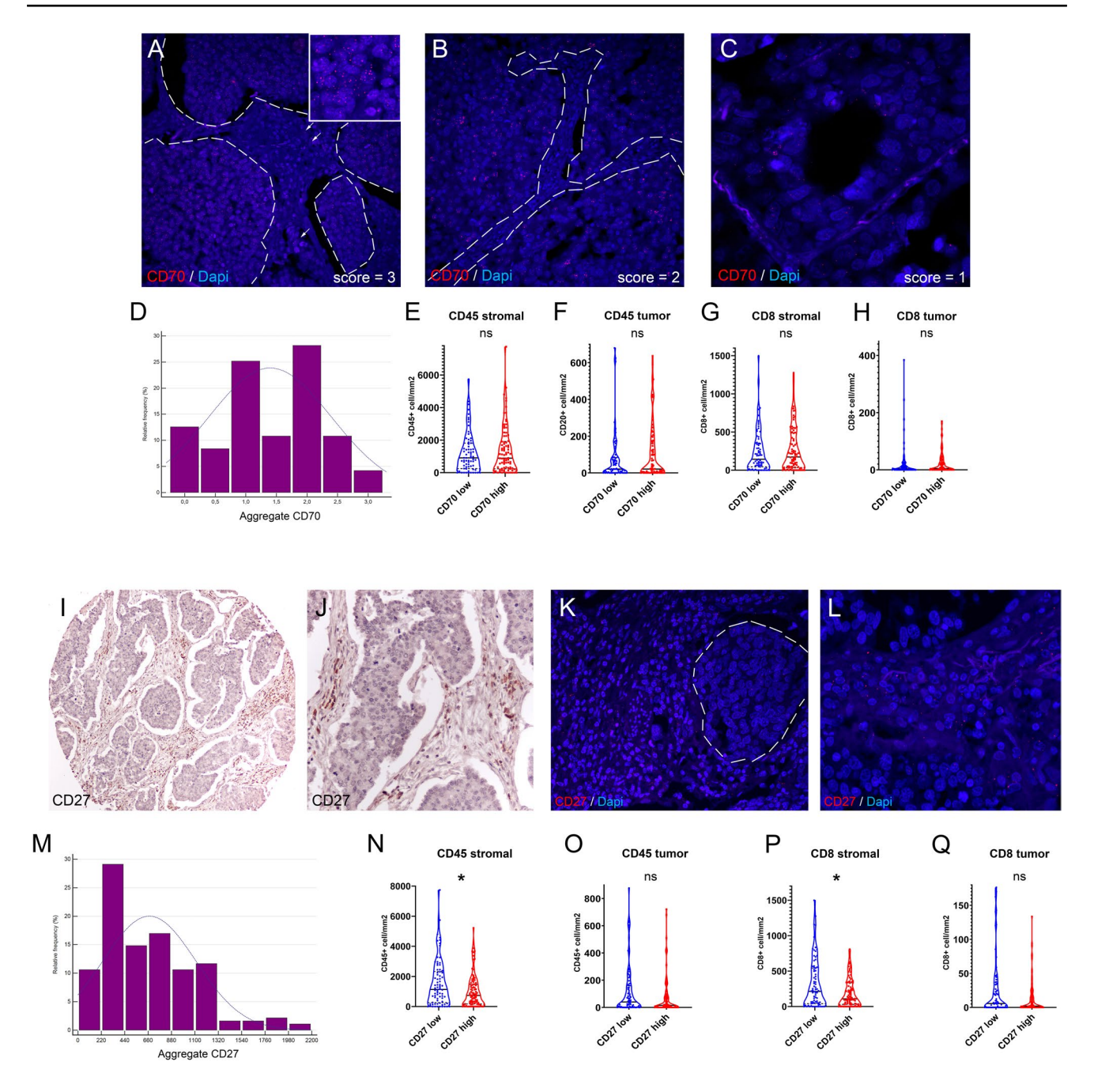


Fig. 2 Expression of CD70 and CD27 in SCLC. RNAscope assays revealed CD70 expression predominantly in tumor nests (A,B, dashed line delimited areas) and scattered in stroma (A, arrows), with most tumors scoring 1.0-2.0 (B,C). Tumors with CD70 scores of 2.0-3.0 were classified as "high," and 0-1.5 as "low." Histogram shows distribution of CD70 scores (D). CD70 expression was not significantly associated with CD45+or CD8+cell densities in stroma or tumor

nests (E-H). CD27 was primarily expressed in stroma (I-L). Distribution of CD27 aggregate scores through tumor samples is shown in panel M. High CD27+cellular density was linked to reduced CD45 + and CD8 + cell densities (N,P), but not in tumor nests (O,Q). Metric data are shown as medians and 95% CI on violin plots. Statistical significance *P<0.05; **P<0.01, ***P<.001. All p values were two-sided

Expression of the CD70/CD27 axis in SCLC TME

To reveal the qualitative expression pattern of the CD70/ CD27 axis in the SCLC TME, we performed double IF stainings for EMT-marker vimentin, pan-macrophage marker CD68, pan-T-cell marker CD3, and B-cell marker CD20. Colocalization studies showed that CD70 protein exhibits a fluke, diffuse signal with a conspicuous complementarity with vimentin staining in tumor nests of CD70high patients (Fig. 4A). Thus, vimentin-positive tumor cell



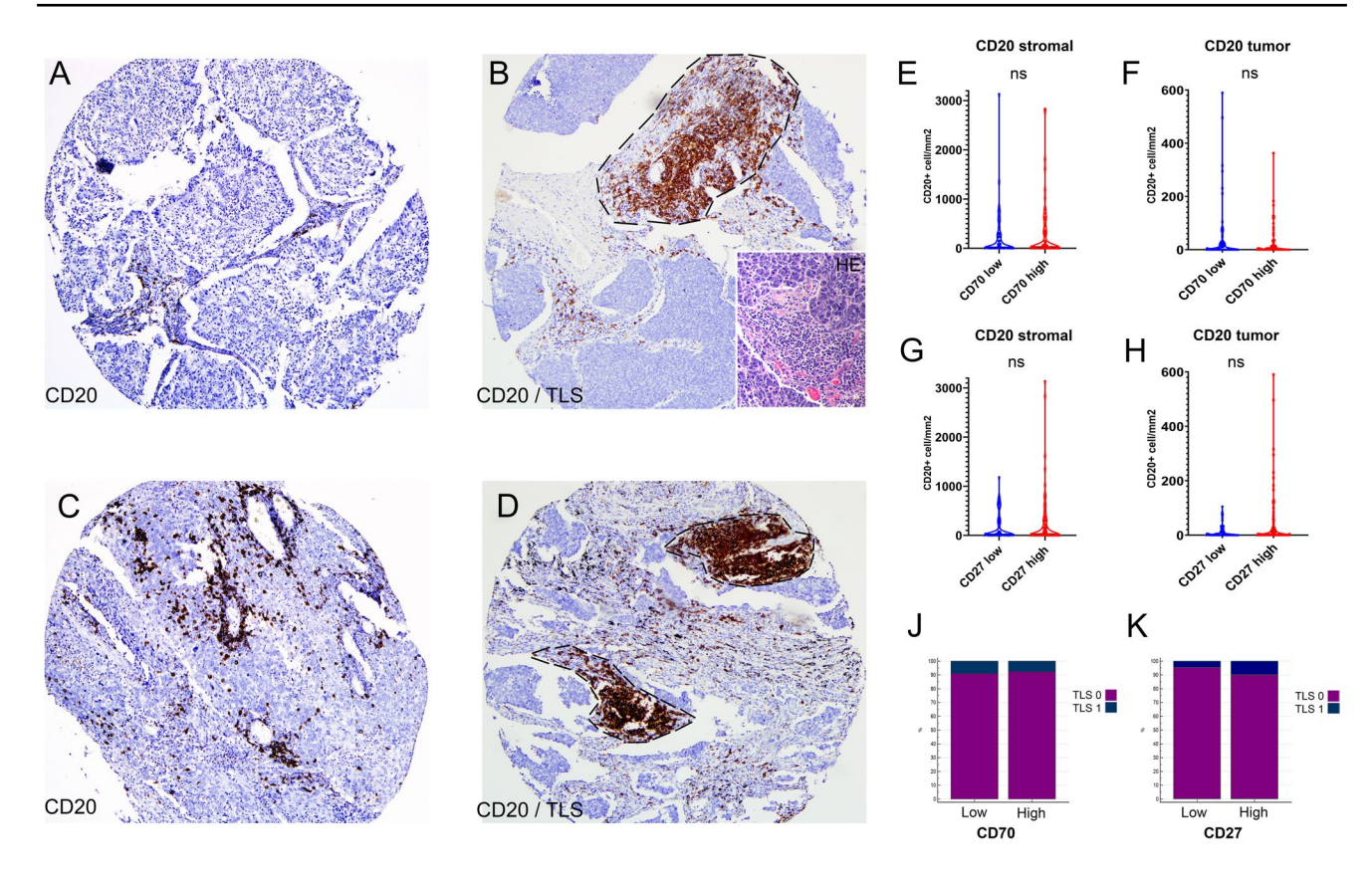


Fig. 3 B-cells in SCLC in the context of the CD70-CD27 axis. CD20+B-cell densities were evaluated in the SCLC cohort using the same scoring method as in the case of CD27. B-cells are primarily located in stromal bands, with occasional intratumoral presence and TLS formation (**A**, **B**). Multiple tumors showed signs of formation of tertiary lymphatic structures (TLSs) made up from congre-

gations of CD20+B-cells (**C,D**, dashed line delimited area). No significant association was found between CD70/CD27 expression and B-cell densities or TLS presence (**E-H, J, K**). Metric data are shown as medians and 95% CI on violin plots. Statistical significance *P < 0.05; **P < 0.01, ***P < .001. All p values were two-sided

clusters show lower levels of CD70-expression indicating that the epithelial phenotype is more associated with checkpoint's expression. In contrast, CD70 was expressed by multiple vimentin-positive CAFs stroma compartment (Fig. 4B, arrow). Among immune cells, the majority of CD68 + TAMs seemed to express CD70 both in the stroma and the intratumoral compartments (Fig. 4C, arrows; **D**, dashed line). When observing tumor samples of CD70high patients, CD3 staining showed that only a fraction of T-cells express the molecule (Fig. 4E,F, arrows), with most CD3 + cells being CD70-negative (Fig. 4F, asterisks). We found that even in CD70-high patient tumors, CD20 + B-cells showed no signs of coexpression with CD70 (Fig. 4G,H, asterisks). As expected, CD27 expression was limited to the TME, with no presence on tumor cells. CD27 showed coexpression with scattered vimentin + CAFs (Fig. 4I, arrow) and CD3 + T-cells (Fig. 4J, arrows) in the stroma, and with a moderate number of CD68 + TAMs in the stroma compartment and inside tumor nests (Fig. 4K, arrows).

CD70 and CD27 expression in the clinical setting

Next, we assessed the clinical relevance of CD70 and CD27 expression in our cohort, where a total of n = 74 patients had eligible CD70 RNAscope score and OS data from which n=51 patients were diagnosed at an early stage (I-II) and a total of n = 81 patients had eligible OS data and CD27 IHC score, from which n = 54 were in the early stage. Stage showed no conspicuous association neither with CD70 expression (p = 0.447), nor with CD27 expression (p=0.945) according to the chi-squared test. Early-stage patients showed significantly increased OS in every setting (p = 0.0002), therefore, we performed all further analysis limited to this subgroup as well. Gender showed no significant association with survival (p = 0.112), but adjuvant chemotherapy administration showed a trend toward increased OS (p = 0.087). We included all three confounders in multivariate analyses.

We found that CD70-high patients exhibited significantly decreased OS (p=0.0078, HR: 1.795 (95% CI, 1.127



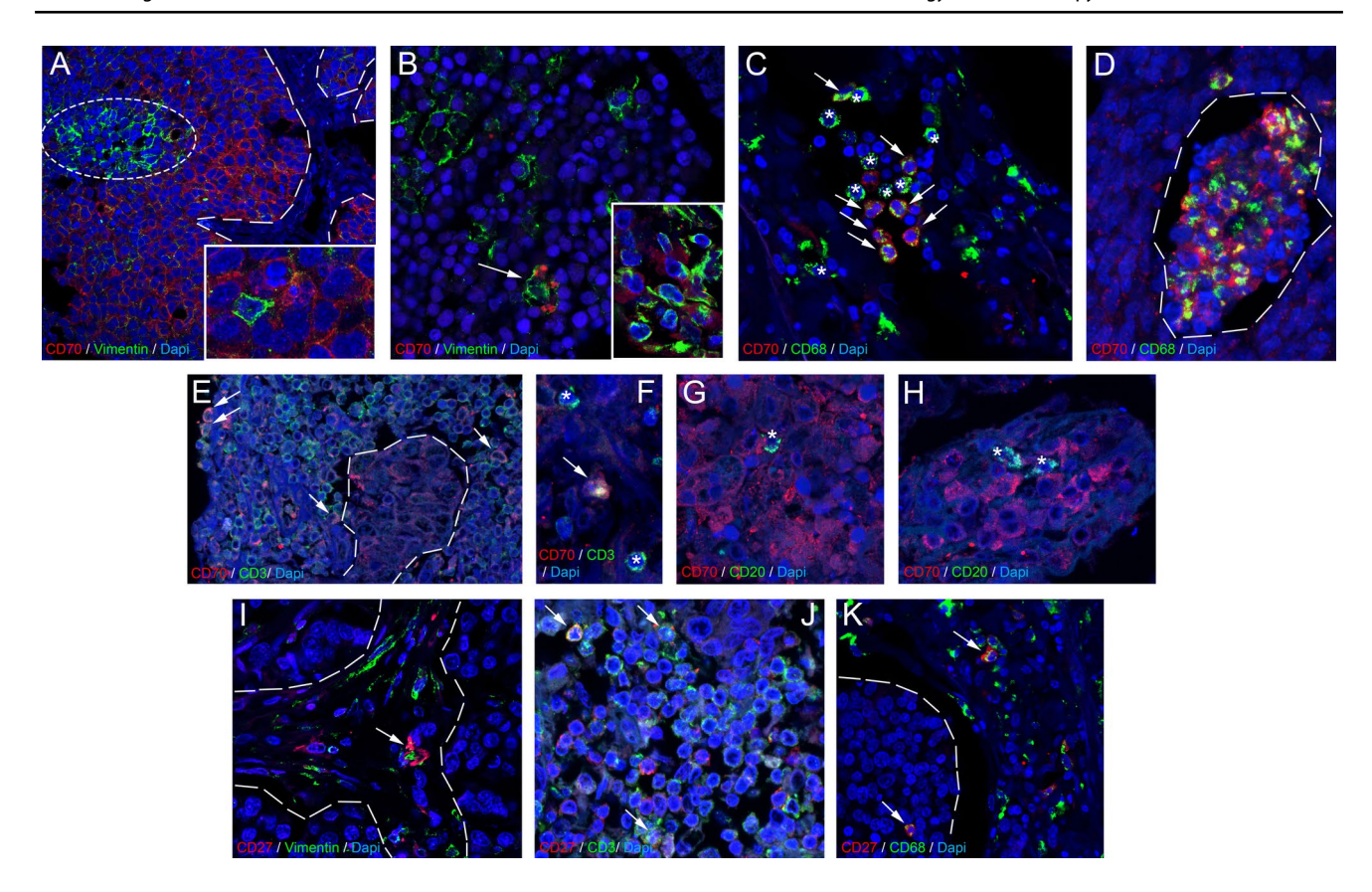


Fig. 4 Coexpression of CD70 and CD27 on TME cells. Double IF staining revealed a diffuse CD70 protein signal in tumor nests, showing complementarity with vimentin in CD70-high patients, with lower CD70 expression in vimentin-positive tumor cells (**A**, ellipsoid area within dashed line delimited area for tumor nest). CD70 was expressed by vimentin-positive CAFs in the stroma (**B**, arrow) and CD68+TAMs in both stroma and tumor nests (**C**, arrows, **D**).

However, not all TAMs showed coexpression (**C**, asterisks). In CD70-high tumors, only a fraction of CD3+T-cells expressed CD70 (**E**,**F**, arrows), while CD20+B-cells showed no coexpression with CD70 (**G**,**H**, asterisks). CD27 was limited to the TME, with occasional vimentin coexpression on CAFs (**I**, arrow). Multiple CD3+T-cells (**J**, arrows), and CD68+TAMs (**K**, arrows) also coexpressed CD27

to 2.861), Fig. 5A), and this difference remained significantly including only early-stage patients (p=0.008. HR: 2.0 (1.146 to 3.49)). Interestingly, when including only immuneoasis tumors according to their CD45 + cellular densities, CD70-high patients still showed inferior OS compared to CD70-low patients (p=0.0346, HR: 2.21 (95% CI, 0.972 to 5.024), Fig. 5B). In contrast, CD70 expression was not prognostic in patients with immune-desert tumors (p=0.115, Fig. 5C).

Next, we assessed the prognostic role of CD27 expression, where a total of n = 81 patients had eligible OS data, from which n = 54 were in the early stage. We found no significant association between CD27 expression and OS, when classifying patients to CD27 high vs low neither in the whole cohort (p = 0.582, Fig. 5D), nor among immune-oasis- (p = 0.382, Fig. 5E), or immune-desert patients (p = 0.209, Fig. 5F). In the contrary, CD20+cellular density was shown to be prognostic in SCLC, where patients with B-cell-infiltrative tumors showed significantly increased OS concerning both their stromal- and

intratumoral B-cell densities (p = 0.0017, HR: 0.491 (95% CI, 0.292 to 0.828), respectively, Fig. 5G,H), with a significant result when assessing only early-stage patients as well (p = 0.0072). Also, patients with TLS present in their tumor samples showed significantly increased OS (p = 0.0323, HR: 0.48 (95% CI, 0.274 to 0.842), Fig. 5I).t

Cox proportional regression showed that stage (p=0.0006), CD70 score (p=0.0064), stromal-(p=0.003) and intratumoral (p=0.0024) CD20 density, and TLS presence (p=0.02) is prognostic, gender (p=0.098) and adjuvant chemotherapy (p=0.086) is borderline prognostic, whereas age (p=0.721) and CD27 score (p=0.607) is not prognostic according to univariate analyses (Table 2). When including data of stromal and intratumoral CD45 + and CD8 + cellular densities from our earlier study on the same cohort (Dora et al., 13), along with all confounders below the significance threshold (p<0.1), multivariate Cox regression showed that only stage (p<0.0001) and CD70 score (p=0.0013) remained as significant prognosticators (Table 2), indicating that in



165

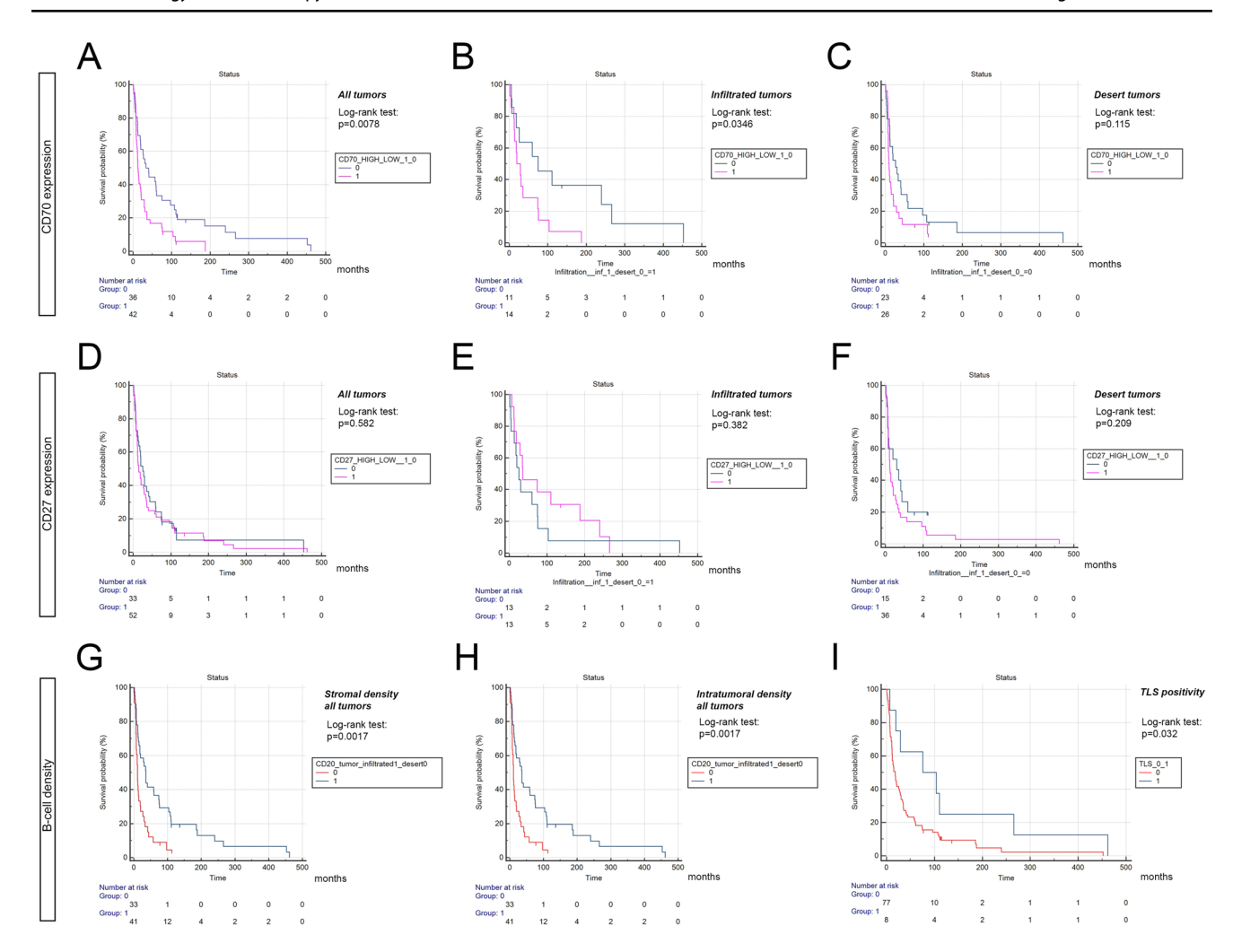


Fig. 5 CD70 and CD27 expression and B-cell densities in the context of overall survival. CD70-high (1) patients showed significantly decreased OS compared to CD70-low (0) patients (p=0.0078, HR: 1.795, **A.** CD70 was also prognostic including only patients with immune-oasis (infiltrated) tumors (p=0.0346, HR: 2.21, **B**, but not in the population with immune-desert tumors (p=0.115, **C**. CD27

(high (1) vs low (0)) expression did not significantly impact OS, neither in the whole cohort **D** nor in the immune-oasis (infiltrated) **E** or desert population **F**. In contrast, B-cell density was prognostic, with increased OS for patients with high (1) stromal/intratumoral B-cell infiltration (p=0.0017, G,H) and TLS presence (1) (p=0.0323, HR: 0.48,I)

the current setting, only stage is a stronger prognostic factor than CD70 expression (Table 2).

Discussion

SCLC is a highly aggressive and challenging malignancy with an alarmingly low survival rate, particularly in advanced stages where the 5-year OS rate remains below 1% [8]. Unlike NSCLC, where biomarkers such as tumor mutation burden (TMB) and PD-L1 have shown predictive value for the response to ICIs, SCLC lacks reliable biomarkers for guiding effective therapies [57]. This absence of predictive biomarkers has resulted only in incremental progress in clinical trials, with modest improvements in

progression-free survival when ICIs are used ([40]; [46]). The CD70-CD27 axis, a ligand-receptor pair in the tumor necrosis factor (TNF) superfamily, plays a crucial role in immune regulation and has been implicated in various hematological malignancies. Dysregulation of this axis within the TME was also associated with tumor progression and immune evasion lately in solid cancers, making it a potential target for new therapeutic strategies in lung cancer. Preclinical study on NSCLC cell lines and tumorbearing mice using a combination of anti-CD70 antibody and chemotherapy showed effective NK-cell mediated tumor cell killing and an enhanced intratumoral infiltration of both T and NK cells, as well as an increase in the ratio of CD8+T cells over Tregs [15]. Furthermore, EMT promoted immune escape by inducing CD70 in NSCLC as shown by [38] and



Table 2 Cox proportional hazard regression

Confounder	Cox (U) p-value	Cox (U) Wald	Cox (U) HR	Cox (M) p-value	Cox (M) Wald	Cox (M) HR
Age	0.721	0.127	0.995	>0.1	,	
Gender (1)	0.098	2.478	0.627	> 0.1		
Stage (1)	0.0006	13.012	2.564	< 0.0001	18.141	3.957
Adjuvant CHT (1)	0.086	2.875	0.662	> 0.1		
CD70 score	0.0064	7.323	1.443	0.0013	10.286	1.629
CD27 score	0.607	0.26	0.999	> 0.1		
stromal CD20	0.003	9.061	0.441	> 0.1		
tumoral CD20	0.0024	9.455	0.451	> 0.1		
TLS (1)	0.02	4.353	0.428	> 0.1		
stromal CD45	0.0238	5.111	0.786	> 0.1		
tumoral CD45	0.189	1.722	0.998	> 0.1		
stromal CD8	0.038	4.289	0.795	> 0.1		
tumoral CD8	0.106	2.607	0.955	> 0.1		

Gender (0=male, 1=female); Stage (0=early stage (I-II), 1=advanced stage (III)); Adjuvant chemotherapy (CHT, 0=not received, 1=received); TLS (0=not present, 1=present). U Univariate analysis with no confounders, M Multivariate analysis with the present confounders plus CD45 and CD8 cellular densities from (Dora et al., 13)

Bold indicates significant results (p<0.05) for Univariate and Multivariate Cox regression

the molecule was also reported to be upregulated in EGFR mutant NSCLC cells that have undergone EMT, where drug-resistant CD70+tumors were successfully targeted with CD70-Antibody-drug-conjugates, CAR-T Cells, and NK-CARs [36]. However, the role of the axis in small cell histologies remains unexplored.

Our findings demonstrated that CD70 and CD27 are expressed in tumor cells and within the TME of SCLC, with distinct expression patterns. CD70 expression was predominantly found within tumor nests and to a lesser extent in the stroma, while CD27 was primarily located in the stromal compartment. Notably, CD70 expression did not correlate with immune cell densities within either the stroma or tumor nests, whereas high CD27 expression was associated with reduced CD45 + and CD8 + cell densities in the stroma. There is no comprehensive expression analysis for CD70 or CD27 currently available in SCLC. Single-cell data indicates that in NSCLC, CD70 expression is mainly confined to CD4+T-cell subsets (especially Tregs) and B-cells, with virtually no macrophage-related expression. In contrast, in SCLC, that was lately described as a cancer with a predominantly macrophage-rich TME ([12]; [13]; [32], [52]), CD70 expression has a strong representation from CD68+TAMs, and the molecule's coexpression on T- or B-cells is not prevalent. This is in line with our previous and currently presented data, namely that most SCLC tumors harbor a low density of T-cells [13] and B-lymphocytes. NSCLC singlecell data are more in line with our stainings on SCLC specimens concerning the expression of CD27 on T-cells, but not in B-cells, where no colocalization was detected between CD20 and CD27. Furthermore, CD27 protein is also present in TAMs, a characteristic that was not described previously in NSCLC.

In SCLC tumors, CD70 exhibited a diffuse signal with lower expression in vimentin-positive tumor cell clusters but was present in vimentin-positive CAFs in the stroma. CD70 was also expressed by the majority of CD68 + TAMs in both the stroma and tumor compartments, while CD3 + T-cells showed limited CD70 expression. CD20 + B-cells did not coexpress CD70. It was previously shown in CRC that CAFs express CD70 and CD70 + CAF density is an independent adverse prognostic marker in CRC. Functionally, CD70-positive CAFs stimulated migration and significantly increased the frequency of naturally occurring Tregs [26]. Other group came to similar conclusions where simultaneous expression of the molecule with the protein periostin on CAFs predicted worse outcomes in patients with CRC [33]. CD70 expression in GBM is known to be coupled with M2-polarized TAM densities, however, no spatial coexpression was explicitly reported ([45], [17]). The strong association of CD70 with immunosuppressive TAMs is particularly interesting, given that the CD70 expression on dendritic cells was also shown to activate anti-tumorigenic CD8 + T-cell subsets in experimental mice [30], suggesting the molecule's context-dependent role in the TME. While multiple studies reported CD70 expression in situ on tumor cells [15], no other detailed break-down of the molecule's TME protein expression pattern is currently available in the scientific literature. In our cohort, CD27 expression was restricted to the TME, showing coexpression with vimentin + CAFs, CD3 + T-cells, and a moderate number



of CD68+TAMs in the stroma and tumor nests. HPA data in NSCLC consistently show CD27 expression limited to the stroma with no apparent tumor cell expression (https://www.proteinatlas.org/ENSG00000139193-CD27. Apart from hematological malignancies and NSCLC, CD27 expression was detected in tumor bearing mice ([9]; RCC ([10]; [44] and nasopharyngeal carcinoma [19] among other cancers [15].

B-cells represent a TME cell type with a generally positive prognostic role [5]. Tumor-infiltrating B cells and developed TLSs have similarly been observed in lung cancer, with their phenotype differing according to the clinical stage and histological subtype [18]. Several studies have found that CD20+B cell infiltration and the presence of TLSs are associated with a favorable prognosis ([1]; [21]; [18]; [31]; [55]) and response to anti-PD1 immunotherapy in NSCLC ([6]; [39]) making the B-cell-related immune contexture an intriguing topic in SCLC, a knowingly immune-desert tumor, with an overwhelmingly immunosuppressive TME. B-cell and TLS distribution has not yet been elucidated in any significant real-word SCLC cohort. In our cohort, both high densities of CD20 + B-cells and the apparent presence of a TLS were associated with significantly increased OS that underlines the prognostic relevance of B-cell infiltration in a previously unstudied cancer such as SCLC.

Clinically, high CD70 expression was associated with significantly decreased OS, particularly in early-stage patients and those with immune-oasis tumors. In contrast, CD27 expression did not show a significant association with OS. Multivariate analysis confirmed that CD70 expression and tumor stage were significant prognostic factors for OS, while CD27 was not. These results are in line with NSCLC, where acknowledged Kaplan-Meier (KM) Plotter tool compiling OS and RNAseq-based expression data from n = 504 patients from multiple cohorts [23] showed that high CD70 expression is associated with decreased OS (p = 0.008, HR:1.49). In contrast, the same analysis for CD27 showed a survival benefit for CD27-high patients (p = 0.0085, HR:0.67). In our cohort, RNAscope-base tissue expression of CD70 was shown to be an even stronger predictor of OS than CD8 + T-cell density, a basic component of the renowned Immunoscore prognostic index [5]. Moreover, when including only immune-hot SCLCs, high CD70 expression was still a significant negative prognosticator, making the biomarker intriguing for this population when administering future immunotherapies.

Limitations of this study include its retrospective, crosssectional nature and the long recruitment period, which is explained by the low number of operable patients and tumor samples available due to disease aggressiveness. Only a limited number of patients were treated with adjuvant chemotherapy, and recruitment was before the initiation of immunotherapies, therefore we could not assess the predictive role of the CD70/CD27 axis in SCLC.

Conclusion

Our study highlights CD70 as a key prognostic marker in SCLC. High CD70 expression, detected predominantly within tumor cells and macrophages, was linked to significantly reduced OS, also when including only early-stage or immune-oasis tumors. Notably, CD70 expression did not correlate with immune cell infiltration, indicating a distinct prognostic role independent of immune contexture. In contrast, CD27 expression was primarily found in the stroma and was not significantly associated with survival. Additionally, increased B-cell density and the presence of TLSs were correlated with improved outcomes. Given that tissue-level expression data of prognostic biomarkers are particularly valuable in this aggressive cancer, our research gives a solid basis for validation and experimental studies in the future to underpin the role of the CD70/CD27 axis in SCLC tumor immunology.

Supplementary Information The online version contains supplementary material available at https://doi.org/10.1007/s00262-025-04006-2.

Author contributions Conceptualization: DD, ZL and BD. Methodology: DD, ZM, IM, ÁP, PT, SMZB, and HY. Software: DD, ZM, PT, DDo and KA. Investigation: DD, ZM, IV, ÁP, PT, SMZB, KA and BR. Resources: DD, CR, FRH, AG, ZVV, ZL and BD. Validation: BR, DDo, BL and GP. Visualization: DD, IV and PT. Data curation: ZM, IV, ÁP, GP and HY. Formal analysis: PT, BL, SMZB, KA and GP. Project Administration: DD, CR, FRH, AG, ZVV, ZL and BD. Supervision: DD, AG, ZVV, ZL and BD. Funding acquisition: DD, ZM, ZVV, ZL and BD. Writing—Original Draft: DD, ZM, PT, ZL and BD. Writing—Review & Editing: all authors.

Funding Open access funding provided by Semmelweis University. BD was supported by the Austrian Science Fund (FWF I3522, FWF 13977, and 14677) and the "BIOSMALL" EU HORIZON-MSCA-2022-SE-01 project. BD and ZM were supported by funding from the Hungarian National Research, Development, and Innovation Office (2020-1.1.6-JÔVŐ, TKP2021-EGA-33, FK-143751 and FK-147045). ZVV, AG, IV, AP were funded by grants from the HUN-REN Hungarian Research Network, Momentum Research Grant from the Hungarian Academy of Sciences (LP-2021-14), Project no. 2022-1.1.1-KK-2022-00005 has been implemented with the support provided by the Ministry of Innovation and Technology of Hungary from the National Research, Development and Innovation Fund. Project no. RRF-2.3.1-21-2022-00003 has been implemented with the support provided by the European Union. ZL acknowledges funding from the Hungarian National Research, Development and Innovation Office (OTKA-FK, #146775). DD acknowledges funding from the Hungarian National Research, Development and Innovation Office (OTKA-PD, #142287). ZM was supported by the New National Excellence Program of the Ministry for Innovation and Technology of Hungary (UNKP-20-3, UNKP-21-3 and UNKP-23-5), and by the Bolyai Research Scholarship of the Hungarian Academy of Sciences. ZM is also the recipient of the International Association for the Study of Lung Cancer/International Lung Cancer Foundation Young Investigator Grant (2022). DD was



supported by the New National Excellence Program of the Ministry for Innovation and Technology of Hungary (UNKP-23–5), and by the Bolyai Research Scholarship of the Hungarian Academy of Sciences.

Data availability All processed data used in this study are available in the manuscript text and supplementary material. Unprocessed data and patient metadata are available upon reasonable request from the corresponding authors.

Declarations

Conflict of interest The authors declare no competing interests.

Ethics approval and consent to participate The study was carried out in accordance with the Helsinki Declaration guidelines of the World Medical Association Hungarian scientific ethics committee (ETT-TUKEB-7214–1/2016/EKU). Due to the retrospective nature of the study, the requirement for individual informed consent was waived. Following the acquisition of clinical data, the patients' identities were anonymized, ensuring that the patients cannot be identified either directly or indirectly.

Consent for publication All authors have reviewed and approved the final version of the manuscript.

Open Access This article is licensed under a Creative Commons Attribution 4.0 International License, which permits use, sharing, adaptation, distribution and reproduction in any medium or format, as long as you give appropriate credit to the original author(s) and the source, provide a link to the Creative Commons licence, and indicate if changes were made. The images or other third party material in this article are included in the article's Creative Commons licence, unless indicated otherwise in a credit line to the material. If material is not included in the article's Creative Commons licence and your intended use is not permitted by statutory regulation or exceeds the permitted use, you will need to obtain permission directly from the copyright holder. To view a copy of this licence, visit http://creativecommons.org/licenses/by/4.0/.

References

- Al-Shibli KI, Donnem T, Al-Saad S, Persson M, Bremnes RM, Busund LT (2008) Prognostic effect of epithelial and stromal lymphocyte infiltration in non-small cell lung cancer. Clin Cancer Res 14(16):5220–5227. https://doi.org/10.1158/1078-0432. CCR-08-0133
- Bankhead P, Loughrey MB, Fernández JA, Dombrowski Y, McArt DG, Dunne PD, McQuaid S, Gray RT, Murray LJ, Coleman HG, James JA, Salto-Tellez M, Hamilton PW (2017) QuPath: open source software for digital pathology image analysis. Sci Rep 7(1):16878. https://doi.org/10.1038/s41598-017-17204-5
- 3. Battifora H (1986) Methods in laboratory investigation. The multitumor (sausage) tissue block: novel method for immunohistochemical antibody testing. Lab Investig 55:244–248
- Bertrand P, Maingonnat C, Penther D, Guney S, Ruminy P, Picquenot JM et al (2013) The costimulatory molecule CD70 is regulated by distinct molecular mechanisms and is associated with overall survival in diffuse large B-cell lymphoma. Genes Chromosom Cancer 52(8):764–774
- 5. Bruni D, Angell HK, Galon J (2020) The immune contexture and Immunoscore in cancer prognosis and therapeutic

- efficacy. Nat Rev Cancer 20(11):662–680. https://doi.org/10.1038/s41568-020-0285-7
- Budczies J, Kirchner M, Kluck K, Kazdal D, Glade J, Allgäuer M, Kriegsmann M, Heußel CP, Herth FJ, Winter H, Meister M, Muley T, Fröhling S, Peters S, Seliger B, Schirmacher P, Thomas M, Christopoulos P, Stenzinger A (2021) A gene expression signature associated with B cells predicts benefit from immune checkpoint blockade in lung adenocarcinoma. Oncoimmunology 10(1):1860586. https://doi.org/10.1080/2162402X.2020.1860586
- Chen B, Khodadoust MS, Liu CL, Newman AM, Alizadeh AA (2018) Profiling tumor infiltrating immune cells with CIBER-SORT. Methods Mol Biol 1711:243–259
- Cittolin-Santos GF, Knapp B, Ganesh B, Gao F, Waqar S, Stinch-combe TE, Govindan R, Morgensztern D (2024) The changing landscape of small cell lung cancer. Cancer 130(14):2453–2461. https://doi.org/10.1002/cncr.35281
- Claus C, Riether C, Schürch C, Matter MS, Hilmenyuk T, Ochsenbein AF (2012) CD27 signaling increases the frequency of regulatory T cells and promotes tumor growth. Cancer Res 72(14):3664
 3676. https://doi.org/10.1158/0008-5472.CAN-11-2791
- Diegmann J, Junker K, Loncarevic IF, Michel S, Schimmel B, von Eggeling F (2006) Immune escape for renal cell carcinoma: CD70 mediates apoptosis in lymphocytes. Neoplasia 8(11):933–938. https://doi.org/10.1593/neo.06451
- Dora D, Rivard C, Yu H, Bunn P, Suda K, Ren S, Lueke Pickard S, Laszlo V, Harko T, Megyesfalvi Z, Moldvay J, Hirsch FR, Dome B, Lohinai Z (2020) Neuroendocrine subtypes of small cell lung cancer differ in terms of immune microenvironment and checkpoint molecule distribution. Mol Oncol. 14(9):1947–1965. https:// doi.org/10.1002/1878-0261.12741
- Dora D, Rivard C, Yu H, Pickard SL, Laszlo V, Harko T, Megyesfalvi Z, Dinya E, Gerdan C, Szegvari G, Hirsch FR, Dome B, Lohinai Z (2021) Characterization of tumor-associated macrophages and the immune microenvironment in limited-stage neuroendocrine-high and -low small cell lung cancer. Biology (Basel) 10(6):502. https://doi.org/10.3390/biology10060502
- Dora D, Rivard C, Yu H, Pickard SL, Laszlo V, Harko T, Megyesfalvi Z, Gerdan C, Dinya E, Hoetzenecker K, Hirsch FR, Lohinai Z, Dome B (2023) Protein expression of immune checkpoints STING and MHCII in small cell lung cancer. Cancer Immunol Immunother 72(3):561–578. https://doi.org/10.1007/ s00262-022-03270-w
- Dora D, Vörös I, Varga ZV, Takacs P, Teglasi V, Moldvay J, Lohinai Z (2023) BRAF RNA is prognostic and widely expressed in lung adenocarcinoma. Transl Lung Cancer Res. 12(1):27–41. https://doi.org/10.21037/tlcr-22-449
- Flieswasser T, Van den Eynde A, Van Audenaerde J et al (2022) The CD70-CD27 axis in oncology: the new kids on the block. J Exp Clin Cancer Res 41:12. https://doi.org/10.1186/ s13046-021-02215-y
- 16. Garon EB, Hellmann MD, Rizvi NA, Carcereny E, Leighl NB, Ahn MJ, Eder JP, Balmanoukian AS, Aggarwal C, Horn L, Patnaik A, Gubens M, Ramalingam SS, Felip E, Goldman JW, Scalzo C, Jensen E, Kush DA, Hui R (2019) Five-year overall survival for patients with advanced non-small-cell lung cancer treated with pembrolizumab: results from the phase I KEYNOTE-001 study. J Clin Oncol 37(28):2518–2527
- 17. Ge H, Mu L, Jin L, Yang C, Chang YE, Long Y, DeLeon G, Deleyrolle L, Mitchell DA, Kubilis PS, Lu D, Qi J, Gu Y, Lin Z, Huang J (2017) Tumor associated CD70 expression is involved in promoting tumor migration and macrophage infiltration in GBM. Int J Cancer 141(7):1434–1444. https://doi.org/10.1002/ijc.30830
- Germain C, Gnjatic S, Tamzalit F, Knockaert S, Remark R, Goc J, Lepelley A, Becht E, Katsahian S, Bizouard G, Validire P, Damotte D, Alifano M, Magdeleinat P, Cremer I, Teillaud JL, Fridman WH, Sautès-Fridman C, Dieu-Nosjean MC (2014)



- Presence of B cells in tertiary lymphoid structures is associated with a protective immunity in patients with lung cancer. Am J Respir Crit Care Med 189(7):832–844. https://doi.org/10.1164/rccm.201309-1611OC
- Gong L, Luo J, Zhang Y, Yang Y, Li S, Fang X, Zhang B, Huang J, Chow LK, Chung D, Huang J, Huang C, Liu Q, Bai L, Tiu YC, Wu P, Wang Y, Tsao GS, Kwong DL, Lee AW, Dai W, Guan XY (2023) Nasopharyngeal carcinoma cells promote regulatory T cell development and suppressive activity via CD70-CD27 interaction. Nat Commun 14(1):1912. https://doi.org/10.1038/s41467-023-37614-6
- Goto N, Tsurumi H, Takemura M, Kanemura N, Kasahara S, Hara T et al (2012) Serum soluble CD27 level is associated with outcome in patients with diffuse large B-cell lymphoma treated with rituximab, cyclophosphamide, doxorubicin, vincristine and prednisolone. Leuk Lymphoma 53(8):1494–1500
- Gottlin EB, Bentley RC, Campa MJ, Pisetsky DS, Herndon JE 2nd, Patz EF Jr (2011) The association of intratumoral germinal centers with early-stage non-small cell lung cancer. J Thorac Oncol 6(10):1687–1690. https://doi.org/10.1097/JTO.0b013e3182 217bec
- Guikema JEJ, Hovenga S, Vellenga E, Conradie JJ, Abdulahad WH, Bekkema R et al (2003) CD27 is heterogeneously expressed in multiple myeloma: low CD27 expression in patients with highrisk disease. Br J Haematol 121(1):36–43
- Győrffy B (2024) Transcriptome-level discovery of survivalassociated biomarkers and therapy targets in non-small-cell lung cancer. Br J Pharmacol 181(3):362–374. https://doi.org/10.1111/ bph.16257
- Horn L, Mansfield AS, Szczęsna A, Havel L, Krzakowski M, Hochmair MJ, Liu SV (2018) First-line atezolizumab plus chemotherapy in extensive-stage small-cell lung cancer. N Engl J Med 379(23):2220–2229
- Inaguma S, Lasota J, Czapiewski P, Langfort R, Rys J, Szpor J et al (2020) CD70 expression correlates with a worse prognosis in malignant pleural mesothelioma patients via immune evasion and enhanced invasiveness. J Pathol 250(2):205–216
- Jacobs J, Deschoolmeester V, Zwaenepoel K, Flieswasser T, Deben C, Van den Bossche J, Hermans C, Rolfo C, Peeters M, De Wever O, Lardon F, Siozopoulou V, Smits E, Pauwels P (2018) Unveiling a CD70-positive subset of cancer-associated fibroblasts marked by pro-migratory activity and thriving regulatory T cell accumulation. Oncoimmunology 7(7):e1440167. https://doi.org/10.1080/2162402X.2018.1440167
- Jacobs J, Deschoolmeester V, Zwaenepoel K, Rolfo C, Silence K, Rottey S et al (2015) CD70: an emerging target in cancer immunotherapy. Pharmacol Ther 155:1–10
- Jacobs J, Zwaenepoel K, Rolfo C, Van den Bossche J, Deben C, Silence K et al (2015) Unlocking the potential of CD70 as a novel immunotherapeutic target for non-small cell lung cancer. Oncotarget 6(15):13462–13475
- Jilaveanu LB, Sznol J, Aziz SA, Duchen D, Kluger HM, Camp RL (2012) CD70 expression patterns in renal cell carcinoma. Hum Pathol 43(9):1394–1399
- Keller AM, Schildknecht A, Xiao Y, van den Broek M, Borst J (2008) Expression of costimulatory ligand CD70 on steady-state dendritic cells breaks CD8+ T cell tolerance and permits effective immunity. Immunity 29(6):934–946. https://doi.org/10.1016/j. immuni.2008.10.009
- Kinoshita T, Muramatsu R, Fujita T, Nagumo H, Sakurai T, Noji S, Takahata E, Yaguchi T, Tsukamoto N, Kudo-Saito C, Hayashi Y, Kamiyama I, Ohtsuka T, Asamura H, Kawakami Y (2016) Prognostic value of tumor-infiltrating lymphocytes differs depending on histological type and smoking habit in completely resected non-small-cell lung cancer. Ann Oncol 27(11):2117–2123. https://doi.org/10.1093/annonc/mdw319

- 32. Klein S, Schulte A, Arolt C, Tolkach Y, Reinhardt HC, Buettner R, Quaas A (2023) Intratumoral abundance of M2-macrophages is associated with unfavorable prognosis and markers of T-cell exhaustion in small cell lung cancer patients. Mod Pathol. 36(10):100272. https://doi.org/10.1016/j.modpat.2023.100272
- Komura M, Wang C, Ito S, Kato S, Ueki A, Ebi M, Ogasawara N, Tsuzuki T, Kasai K, Kasugai K, Takiguchi S, Takahashi S, Inaguma S (2024) Simultaneous expression of CD70 and POSTN in cancer-associated fibroblasts predicts worse survival of colorectal cancer patients. Int J Mol Sci 25(5):2537. https://doi.org/10.3390/ iims25052537
- Kong F, Ye Q, Xiong Y (2023) Comprehensive analysis of prognosis and immune function of CD70-CD27 signaling axis in pancancer. Funct Integr Genomics 23:48. https://doi.org/10.1007/s10142-023-00977-6
- Liu N, Sheng X, Liu Y, Zhang X, Yu J (2013) Increased CD70 expression is associated with clinical resistance to cisplatin-based chemotherapy and poor survival in advanced ovarian carcinomas. Onco Targets Ther 6:615–619
- Nilsson MB, Yang Y, Heeke S, Patel SA, Poteete A, Udagawa H, Elamin YY, Moran CA, Kashima Y, Arumugam T, Yu X, Ren X, Diao L, Shen L, Wang Q, Zhang M, Robichaux JP, Shi C, Pfeil AN, Tran H, Gibbons DL, Bock J, Wang J, Minna JD, Kobayashi SS, Le X, Heymach JV (2023) CD70 is a therapeutic target upregulated in EMT-associated EGFR tyrosine kinase inhibitor resistance. Cancer Cell 41(2):340-355.e6. https://doi.org/10.1016/j.ccell.2023.01.007
- 37. Nolte MA, Arens R, van Os R, van Oosterwijk M, Hooibrink B, van Lier RAW et al (2005) Immune activation modulates hematopoiesis through interactions between CD27 and CD70. Nat Immunol 6(4):412–418
- 38. Ortiz-Cuaran S, Swalduz A, Foy JP, Marteau S, Morel AP, Fauvet F, De Souza G, Michon L, Boussageon M, Gadot N, Godefroy M, Léon S, Tortereau A, Mourksi NE, Leonce C, Albaret MA, Dongre A, Vanbervliet B, Robert M, Tonon L, Pommier RM, Hofman V, Attignon V, Boyault S, Audoynaud C, Auclair J, Bouquet F, Wang Q, Ménétrier-Caux C, Pérol M, Caux C, Hofman P, Lantuejoul S, Puisieux A, Saintigny P (2022) Epithelial-tomesenchymal transition promotes immune escape by inducing CD70 in non-small cell lung cancer. Eur J Cancer 169:106–122. https://doi.org/10.1016/j.ejca.2022.03.038
- Patil NS, Nabet BY, Müller S, Koeppen H, Zou W, Giltnane J, Au-Yeung A, Srivats S, Cheng JH, Takahashi C, de Almeida PE, Chitre AS, Grogan JL, Rangell L, Jayakar S, Peterson M, Hsia AW, O'Gorman WE, Ballinger M, Banchereau R, Shames DS (2022) Intratumoral plasma cells predict outcomes to PD-L1 blockade in non-small cell lung cancer. Cancer Cell 40(3):289-300.e4. https://doi.org/10.1016/j.ccell.2022.02.002
- 40. Paz-Ares L, Chen Y, Reinmuth N, Hotta K, Trukhin D, Statsenko G, Hochmair MJ, Özgüroğlu M, Ji JH, Garassino MC, Voitko O, Poltoratskiy A, Musso E, Havel L, Bondarenko I, Losonczy G, Conev N, Mann H, Dalvi TB, Jiang H, Goldman JW (2022) Durvalumab, with or without tremelimumab, plus platinum-etoposide in first-line treatment of extensive-stage small-cell lung cancer: 3-year overall survival update from CASPIAN. ESMO Open. 7(2):100408. https://doi.org/10.1016/j.esmoop.2022.100408
- Paz-Ares L, Dvorkin M, Chen Y, Reinmuth N, Hotta K, Trukhin D, Williamson M (2019) Durvalumab plus platinum–etoposide versus platinum–etoposide in first-line treatment of extensive-stage small-cell lung cancer (CASPIAN): a randomised, controlled, open-label, phase 3 trial. The Lancet 394(10212):1929–1939
- Petrau C, Cornic M, Bertrand P, Maingonnat C, Marchand V, Picquenot J-M et al (2014) CD70: a potential target in breast Cancer?
 J Cancer 5(9):761–764
- 43. Phillips T, Barr PM, Park SI, Kolibaba K, Caimi PF, Chhabra S et al (2019) A phase 1 trial of SGN-CD70A in patients with



- CD70-positive diffuse large B cell lymphoma and mantle cell lymphoma. Investig New Drugs 37(2):297–306
- Pich C, Sarrabayrouse G, Teiti I, Mariamé B, Rochaix P, Lamant L, Favre G, Maisongrosse V, Tilkin-Mariamé AF (2016) Melanoma-expressed CD70 is involved in invasion and metastasis. Br J Cancer. 114(1):63–70. https://doi.org/10.1038/bjc.2015.412
- Pratt D, Pittaluga S, Palisoc M, Fetsch P, Xi L, Raffeld M, Gilbert MR, Quezado M (2017) Expression of CD70 (CD27L) is associated with epithelioid and sarcomatous features in IDH-wild-type glioblastoma. J Neuropathol Exp Neurol 76(8):697–708. https://doi.org/10.1093/jnen/nlx051
- Remon J, Aldea M, Besse B, Planchard D, Reck M, Giaccone G, Soria JC (2021) Small cell lung cancer: a slightly less orphan disease after immunotherapy. Ann Oncol 32(6):698–709. https://doi.org/10.1016/j.annonc.2021.02.025
- 47. Riether C, Pabst T, Höpner S, Bacher U, Hinterbrandner M, Banz Y, Müller R, Manz MG, Gharib WH, Francisco D, Bruggmann R, van Rompaey L, Moshir M, Delahaye T, Gandini D, Erzeel E, Hultberg A, Fung S, de Haard H, Leupin N, Ochsenbein AF (2020) Targeting CD70 with cusatuzumab eliminates acute myeloid leukemia stem cells in patients treated with hypomethylating agents. Nat Med 26(9):1459–1467. https://doi.org/10.1038/s41591-020-0910-8
- Riether C, Schurch CM, Buhrer ED, Hinterbrandner M, Huguenin A-L, Hoepner S et al (2017) CD70/CD27 signaling promotes blast stemness and is a viable therapeutic target in acute myeloid leukemia. J Exp Med 214(2):359–380
- Riether C, Schürch CM, Flury C, Hinterbrandner M, Drück L, Huguenin AL, Baerlocher GM, Radpour R, Ochsenbein AF (2015) Tyrosine kinase inhibitor-induced CD70 expression mediates drug resistance in leukemia stem cells by activating Wnt signaling. Sci Transl Med. 7(298):298ra119. https://doi.org/10.1126/scitranslmed.aab1740
- Sauer T, Parikh K, Sharma S, Omer B, Sedloev D, Chen Q, Angenendt L, Schliemann C, Schmitt M, Müller-Tidow C, Gottschalk S, Rooney CM (2021) CD70-specific CAR T cells have potent activity against acute myeloid leukemia without HSC toxicity. Blood 138(4):318–330. https://doi.org/10.1182/blood. 2020008221
- Seyfrid M, Maich WT, Shaikh MV et al (2022) CD70 as an actionable immunotherapeutic target in recurrent glioblastoma and its microenvironment. J Immunother Cancer 10:e003289. https://doi.org/10.1136/jitc-2021-003289
- 52. Tosi A, Lorenzi M, Del Bianco P, Roma A, Pavan A, Scapinello A, Resi MV, Bonanno L, Frega S, Calabrese F, Guarneri V, Rosato A, Pasello G (2024) Extensive-stage small-cell lung cancer in patients receiving atezolizumab plus carboplatin-etoposide: stratification of outcome based on a composite score that combines

- gene expression profiling and immune characterization of microenvironment. J Immunother Cancer 12(7):e008974. https://doi. org/10.1136/jitc-2024-008974
- 53. Uhlén M, Fagerberg L, Hallström BM, Lindskog C, Oksvold P, Mardinoglu A, Sivertsson Å, Kampf C, Sjöstedt E, Asplund A, Olsson I, Edlund K, Lundberg E, Navani S, Szigyarto CA, Odeberg J, Djureinovic D, Takanen JO, Hober S, Alm T, Edqvist PH, Berling H, Tegel H, Mulder J, Rockberg J, Nilsson P, Schwenk JM, Hamsten M, von Feilitzen K, Forsberg M, Persson L, Johansson F, Zwahlen M, von Heijne G, Nielsen J (2015) Tissue-based map of the human proteome. Science. 347(6220):1260419. https://doi.org/10.1126/science.1260419
- 54. van Oers MH, Pals ST, Evers LM, van der Schoot CE, Koopman G, Bonfrer JM et al (1993) Expression and release of CD27 in human B-cell malignancies. Blood 82(11):3430–3436
- Weng Y, Yuan J, Cui X, Wang J, Chen H, Xu L, Chen X, Peng M, Song Q (2024) The impact of tertiary lymphoid structures on tumor prognosis and the immune microenvironment in non-small cell lung cancer. Sci Rep 14(1):16246. https://doi.org/10.1038/s41598-024-64980-y
- Wiesmann A, Phillips RL, Mojica M, Pierce LJ, Searles AE, Spangrude GJ et al (2000) Expression of CD27 on murine hematopoietic stem and progenitor cells. Immunity 12(2):193–199
- Yu L, Lai Q, Gou L, Feng J, Yang J (2021) Opportunities and obstacles of targeted therapy and immunotherapy in small cell lung cancer. J Drug Target 29(1):1–11. https://doi.org/10.1080/ 1061186X.2020.1797050
- 58. Zilionis R, Engblom C, Pfirschke C, Savova V, Zemmour D, Saatcioglu HD, Krishnan I, Maroni G, Meyerovitz CV, Kerwin CM, Choi S, Richards WG, De Rienzo A, Tenen DG, Bueno R, Levantini E, Pittet MJ, Klein AM (2019) Single-cell transcriptomics of human and mouse lung cancers reveals conserved myeloid populations across individuals and species. Immunity. 50(5):1317–1334. https://doi.org/10.1016/j.immuni.2019.03.009
- 59. Reck M, Dziadziuszko R, Sugawara S, Kao S, Hochmair M, Huemer F, de Castro Jr G, Havel L, Caro RB, Losonczy G, Lee JS, Kowalski DM, Andric Z, Califano R, Veatch A, Gerstner G, Batus M, Morris S, Kaul M, Cuchelkar V, Li H, Danner BJ, Nabet BY, Liu SV (2024) Five-year survival in patients with extensive-stage small cell lung cancer treated with atezolizumab in the Phase III IMpower133 study and the Phase III IMbrella A extension study. Lung Cancer. 1(196):107924

Publisher's Note Springer Nature remains neutral with regard to jurisdictional claims in published maps and institutional affiliations.

Authors and Affiliations

- Balazs Dome balazs.dome@meduniwien.ac.at

- Department of Anatomy, Histology, and Embryology, Faculty of Medicine, Semmelweis University, Budapest, Hungary
- Department of Tumor Biology, National Koranyi Institute of Pulmonology, Budapest, Hungary



- Division of Thoracic Surgery, Department of Surgery, Comprehensive Cancer Center, Medical University of Vienna, Waehringer Guertel 18-20, 1090 Vienna, Austria
- Department of Thoracic Surgery, Semmelweis University and National Institute of Oncology, Budapest, Hungary
- Cardiometabolic and HUN-REN-SU System Pharmacology Research Group, Department of Pharmacology and Pharmacotherapy, Semmelweis University, Budapest, Hungary
- ⁶ Center for Pharmacology and Drug Research and Development, Semmelweis University, Budapest, Hungary
- Department of Pharmacology and Pharmacotherapy, HCEMM-SU Cardiometabolic Immunology Research Group, Budapest, Hungary

- MTA-SE Momentum Cardio-Oncology and Cardioimmunology Research Group, Budapest, Hungary
- Translational Medicine Institute, Semmelweis University, Tűzoltó Utca 37-47, 1094 Budapest, Hungary
- Division of Medical Oncology, University of Colorado Anschutz Medical Campus, Aurora, USA
- Center for Thoracic Oncology, Tisch Cancer Institute, Mount Sinai Health System, New York, USA
- Department of Pharmacology and Pharmacotherapy, Semmelweis University, Budapest, Hungary

